SPE 102913

Robust Waterflooding Optimization of Multiple Geological Scenarios

G.M. van Essen, SPE; M.J. Zandvliet, SPE; P.M.J. Van den Hof; O.H. Bosgra, Delft U. Of Technology; J.D. Jansen, SPE, Delft U. Of Technology and Shell Int. E&P

This paper was prepared for presentation at the 2006 SPE Annual Technical Conference and Exhibition held in San Antonio, Texas, U.S.A., 24–27 September 2006.

Abstract

Dynamic optimization of waterflooding using optimal control theory has a significant potential to increase ultimate recovery, as has been shown in various studies. However, optimal control strategies often lack robustness to geological uncertainties. We present an approach to reduce the impact of geological uncertainties in the field development phase known as a robust optimization (RO). RO uses a set of realizations that reflect the range of possible geological structures honoring the statistics of the geological uncertainties.

In our study we used 100 realizations of a 3-dimensional reservoir in a fluvial depositional environment with known main flow direction. We optimized the rates of the 8 injection and 4 production wells over the life of the reservoir, with the objective to maximize the average net present value (NPV). We used a gradient-based optimization method where the gradients are obtained with an adjoint formulation.

We compared the results of the RO procedure to two alternative approaches: a nominal optimization and a reactive control approach. The nominal optimization is based on a single realization, while in the reactive approach each production well is shut in when production is no longer profitable. The three control strategies were applied to each realization, from which the average NPV's and three cumulative distribution functions were determined. The RO results displayed a much smaller variance than the alternatives, indicating the increased robustness to geological uncertainty. Moreover, the RO procedure significantly improved the average NPV, compared to the alternative methods: on average 9% higher than using reactive control and 3% higher than for the nominal case.

Introduction

Within this paper, we consider the secondary recovery phase of a petroleum reservoir using waterflooding. In this case a number of injection and production wells are drilled to preserve a steady reservoir pressure and sweep the reservoir. The use of smart wells expands the possibilities to manipulate and control fluid flow paths through the oil reservoir. The ability to manipulate (to some degree) the progression of the oil-water front provides the possibility to search for a control strategy that will result in maximization of ultimate oil recovery. Dynamic optimization of waterflooding using optimal control theory has a significant potential to increase ultimate recovery by delaying water breakthrough and increasing sweep, as has been shown in various studies[1].

However, optimal control strategies often lack robustness to geological uncertainties. By discarding these uncertainties, bounding the sensitivity to a possibly large system-model mismatch is not taken into account within the optimization procedure. As a result, the optimal control strategy may seize to be optimal or may even result into very poor performance.

Dealing with uncertainty is a topic encountered in many fields related to modeling and control. It can essentially be divided into two different strategies, which are not mutually exclusive: reducing the uncertainty *itself* using measurements, i.e. history matching[2,3] and reducing the *sensitivity* to the uncertainty. However, within this paper, we consider a situation in which no production data is assumed available, which rules out any history matching approach to reduce the geological uncertainty. Our study forms part of a larger research project to enable closed-loop model-based reservoir management[4].

A suggested approach from the downstream process industry, to optimization problems which suffer from vast uncertainty and limited measurement information, is the use of a so-called *robust optimization* technique[5,6,7]. In robust optimization, the optimization procedure is carried out over a set of realizations, in this way actively accounting for the influence of the uncertainty. The implementation of multiple realizations within the optimization process has been addressed in Yeten *et al.* (2002), however this study deviates in way they are incorporated in the objective function and in the number of realizations.

The goal of this paper is to present a robust optimization procedure based on a set of 100 realizations of a 3-dimensional oil-water reservoir, which leads to a control strategy that explicitly accounts for geological uncertainty.

Theory

Optimal Control

We consider an optimal control problem in which the injection flow rates and production flow rates are manipulated directly, i.e. a rate-constrained scenario. The objective to optimizing the oil recovery is represented by the maximization of the net present value (NPV) of the cumulative oil production over a fixed time horizon without a discount factor. The objective function (or cost function) is thus given by[1]:

$$J = \sum_{k=1}^{K} \Delta t_k \left[r_o \cdot \boldsymbol{q}_{o,k} - r_w \cdot \boldsymbol{q}_{w,k} - r_i \cdot \boldsymbol{q}_{i,k} \right], \qquad (1)$$

where r_o is the oil revenue [$/m^3], r_w the water production costs [$/m^3] and r_i the water injection costs [$/m^3], which are all assumed constant. The term K presents the total number of time steps k and Δt_k the time interval of time step k in [*day*]. The terms $q_{o,k}$ represents the total flow rate of produced oil [m^3/day], $q_{w,k}$ the total flow rate of produced water [m^3/day] and $q_{i,k}$ the total flow rate of injected water [m^3/day], at time step index k.

The optimization problem involves finding the optimal injection and production flow rates $\boldsymbol{q}^*$ that maximize the performance measure J, while honoring the dynamic system equations. We use a gradient-based optimization algorithm to converge to the (possibly locally) optimal flow rates. The gradients $\frac{\partial J}{\partial \boldsymbol{q}}$ are obtained by solving a system of adjoint equation as described in Brouwer and Jansen (2004) and Sarma *et al*. (2005). Appendix A provides a description of the adjoint-based method to obtain the gradient information.
The gradients $\frac{\partial J}{\partial \boldsymbol{q}}$ are used in a steepest descent algorithm to iteratively converge to the optimal input trajectory:

$$\boldsymbol{q}^{n+1} = \boldsymbol{q}^n + \tau \cdot \frac{\partial J}{\partial \boldsymbol{q}}, \qquad (2)$$

where τ is the step size of the algorithm. We use a fixed step size τ. A line search to find the direction of the greatest descent will speed up convergence, however as this study is not aimed at improving on convergence speed, a fixed τ is used for simplicity reasons.

Using Eq. (2), a situation may occur in which the new flow rates $\boldsymbol{q}^{n+1}$ do not obey Eq. (13) and Eq. (14), as they were discarded in the Hamiltonian function Eq. (15). In order to ensure that they comply with the constraints, a feasible search direction $\boldsymbol{d}$ of the gradient vector $\frac{\partial J}{\partial \boldsymbol{q}}$ needs to be determined. Sarma *et al.* (2006) propos a rather complicated method to obtain feasible directions if there are state constraints. However, as we are dealing with *linear* equality and inequality constraints on the *input variables only*, we can simply apply the *gradient projection method* as described in Luenberger (1984), to determine $\boldsymbol{d}$.

Using $\boldsymbol{d}$, the steepest descent algorithm thus becomes:

$$\boldsymbol{q}^{n+1} = \boldsymbol{q}^n + \tau \cdot \boldsymbol{d}, \qquad (3)$$

Determining the feasible search direction $\boldsymbol{d}$ however does still not guarantee that $\boldsymbol{q}^{n+1}$ is feasible, given the fixed step size τ. It merely ensures that a certain $\tau > 0$ exists for which it is feasible. For this reason, after $\boldsymbol{d}$ is determined, it is subsequently checked for its feasibility. If not the case, τ is scaled down until a feasible $\boldsymbol{q}^{n+1}$ is reached.

Geological Scenarios

The need to model uncertainty is an inevitable result of the modeling process itself; it is simply impractical or impossible to capture all dynamics and properties of a real dynamical system. Adopting a single "uncertain" model description in a model-based control scheme however, does not always create problems. The modeling error may be small and output and measurement data can be used to correct the predicted state and parameter values to their "real" values.

Unfortunately, this does not hold for control strategies based on reservoir models. The geological uncertainty is generally profound, due to the noisy and sparse nature of seismic data, core samples and borehole logs. Besides, during production this uncertainty can be reduced only marginally, as the measurement and output data provide only limited information on the real values of the (large number of) states and model parameters.

The consequence of a large number of uncertain model parameters ($\boldsymbol{\theta}$) is the broad range of possible models that may satisfy the seismic and core sample data. Nevertheless, in many cases a single reservoir model is adopted for simplicity reasons, in which the uncertain parameters $\boldsymbol{\theta}$ are converted to deterministic parameters $\boldsymbol{\alpha}$ by taking their expected values, i.e. $\boldsymbol{\alpha} := E[\boldsymbol{\theta}]$. However, as we are looking at the NPV (denoted by J) as a measure of performance, we are far more interested in the *expected NPV* over the uncertainty space $\boldsymbol{\Theta}$ (spanned by the uncertain parameters $\boldsymbol{\theta}$). It should be noted that this is generally not the same as taking the expected value of the uncertain parameters, i.e.:

$$E_{\boldsymbol{\theta}}\left[J\left(\boldsymbol{q}, \boldsymbol{\theta}\right) \right] \neq J\left(\boldsymbol{q}, E_{\boldsymbol{\theta}}\left[\boldsymbol{\theta}\right]\right), \quad \boldsymbol{\theta} \in \boldsymbol{\Theta}. \qquad (4)$$

A better approximation of the expected NPV may be obtained by discretizing the uncertainty space $\boldsymbol{\Theta}$, resulting in a finite number (N_R) of realizations of $\boldsymbol{\theta}$ and calculating the expected value over the discretized uncertainty space:

$$E_{\boldsymbol{\theta}}\left[J\left(\boldsymbol{q}, \boldsymbol{\theta}\right) \right] \approx E_{\boldsymbol{\theta}_d}\left[J\left(\boldsymbol{q}, \boldsymbol{\theta}_d\right) \right], \quad \boldsymbol{\theta}_d := \left\{ \boldsymbol{\theta}_1, \ldots, \boldsymbol{\theta}_{N_R} \right\}, \qquad (5)$$

where $\boldsymbol{\theta}_d$ is the finite set of (deterministic) realizations of $\boldsymbol{\theta}$. Generally, the realizations are equiprobable, in which case the right-hand side of Eq. (5) is simply the average of the J's, given by:

$$E_{\boldsymbol{\theta}_d}\left[J\left(\boldsymbol{q}, \boldsymbol{\theta}_d\right) \right] = \frac{1}{N_R} \sum_{i=1}^{N_R} J\left(\boldsymbol{q}, \boldsymbol{\theta}_i\right). \qquad (6)$$

If we assume the modeling uncertainty is limited to uncertainty caused by a lack of information on the true geological structure of the reservoir, the realizations of $\boldsymbol{\theta}$ are usually referred to as *geological scenarios*. Different methods are available to create an ensemble of geological scenarios. Using more conventional methods, a geologist may create a number of scenarios based on his own knowledge and experience with comparable reservoirs. The uncertainty space thus provides the geologist with the boundaries within which he can design possible realizations. The advantage of such a method is that geological realism of the scenarios is guaranteed. It is however a rather subjective process, as a result of which the set may be biased. A geostatistics based method, like multiple-point geostatistics[11,14], incorporates statistical information on geological parameters and consequently does not suffer from this problem. It is however harder to generate geologically realistic structures in this manner.

Robust Optimization

The use of an ensemble of geological scenarios to determine the expected revenues from a reservoir, given a specified production strategy is not uncommon. Implementing such an ensemble in an optimization scheme has however not yet found its way into oil recovery optimization methods. Using a set of realizations to account for the impact of uncertainty within optimization problems, which suffer from uncertainty and limited measurement information, is not uncommon in the downstream industry. These optimization procedures are referred to as *robust optimization* (RO) techniques.

Within robust optimization, the set of realizations may be used in different ways to account for the impact of uncertainty. These different approaches are represented by so-called robust optimization *objectives*[4,6,7].

The most straightforward RO objective is using the expected outcome over the set of realizations, which is in our case equal to Eq. (6) in the previous section. Other objectives may involve incorporating the variance of the outcomes or a worst case approach. In this work however, we limit ourselves to the expected NPV, represented by the robust objective function $\bar{J}$.

$$\bar{J}(q) = \frac{1}{N_R}\sum_{i=1}^{N_R} J(q,\theta_i) \quad (7)$$

This results in the following robust optimization problem:

$$\max_q \bar{J}(q) = \max_q \left(\frac{1}{N_R}\sum_{i=1}^{N_R} J(q,\theta_i) \right) \quad (8)$$

From this formulation follows that calculating the expected NPV ($\bar{J}$) involves a linear operation. As a result, calculating the gradients of Eq. (8) involves a linear operation of the gradients of each realization:

$$\frac{\partial \bar{J}}{\partial q} = \frac{1}{N_r}\sum_{r=1}^{N_r} \frac{\partial J_r}{\partial q} \quad (9)$$

The fact that calculating the "mean" gradients $\frac{\partial \bar{J}}{\partial q}$ involves a linear operation has the advantage that the gradients of each realization can be determined separately. As a result, the gradients can be calculated in a sequential manner instead of simultaneously, which would result in a considerable computational burden, limiting the number of realizations to be used. Calculating the gradients sequentially solves this problem, but it does lead to an extended simulation time by a factor N_r. However, the fact that the calculations are decoupled allows for parallel calculations on multiple computers.

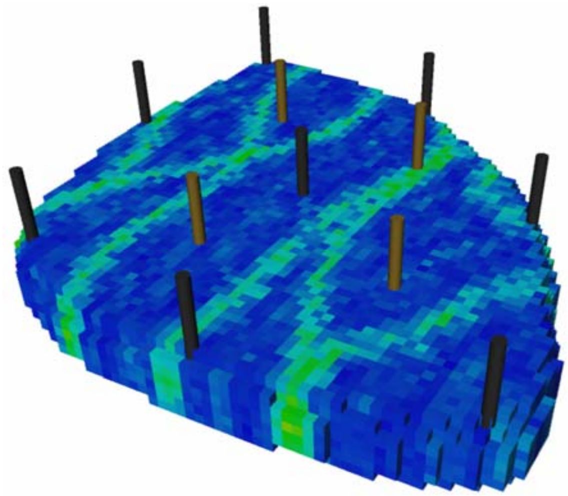

Fig. 1: Example: Permeability field and well locations of realization number 1 of a set of 100 realizations.

Example

We consider a waterflooding example of a 3-dimensional oil-water reservoir model, containing 8 injection wells and 4 production wells over a time horizon of 10 years. It is modeled with 18.553 grid blocks of dimension $8m\times8m\times4m$, and there are 7 vertical layers. The remaining geological and fluid properties used in this example are presented in Table 1. The minimum rate for each well is chosen equal to 0.02 [m^3/day], as setting the rate equal to 0 [m^3/day] presents numerical problems when solving the system of adjoint equation. The maximum rate for each well is fixed at a rate of 160 [m^3/day]. The reservoir is located in a fluvial depositional environment with known main flow direction. Seismic and core sample data is assumed to provide no specific knowledge on the meandering structure of the fluvial depositions. This lack of information on the "real" subsurface structures is assumed to be the major contributor to geological uncertainty.

A set of 100 equiprobable geological scenarios of the reservoir was generated, based on geological insight rather than a geostatistical method. It represents the range of possible geological structures, within the boundaries of the geological uncertainties. One of these scenarios is assumed to be (a close approximation) of the true reservoir. Which one however is unknown.

TABLE 1 – GEOLOGICAL AND FLUID PROPERTIES EXAMPLE

Φ	0.20	[-]
ρ_o (1 bar)	1000	[kg/m^3]
ρ_w (1 bar)	1000	[kg/m^3]
c_o	10^{-5}	[$1/bar$]
c_w	10^{-5}	[$1/bar$]
μ_o	10^{-3}	[$Pa\ s$]
μ_w	10^{-3}	[$Pa\ s$]
$p(0)$	400	[bar]
$S(0)$	0.10	[-]
p_{cow}	0	[bar]

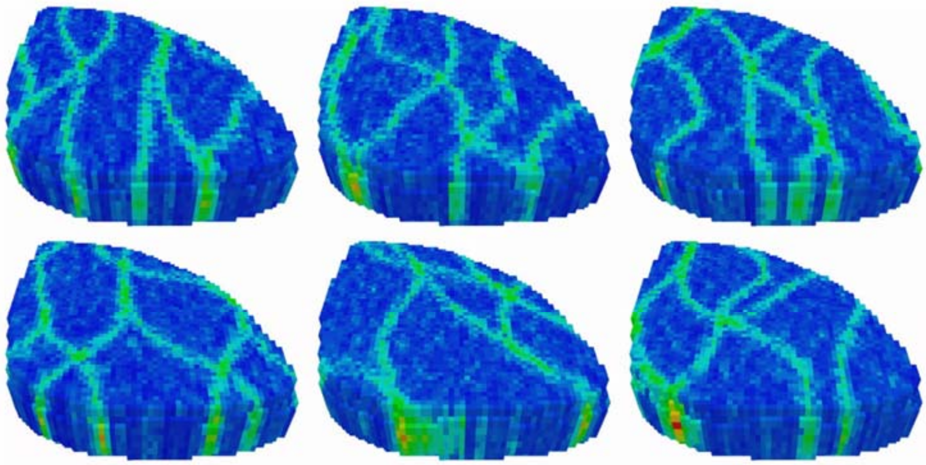

Fig. 2: Permeability field of 6 (randomly chosen) realizations out of a set of 100, showing alternative fluvial structures. The realizations are assumed to have equal probability of occurance.

The absolute permeability field and well locations of the first realization of the set is depicted in Fig. 1. Fig. 2 displays the absolute permeability field of a selection of realizations frm the set without the wells.

We consider 3 different production strategies: a reactive approach, a nominal optimization approach using only one realization and a robust optimization approach using the entire set of realizations. Their performance is evaluated using the objective function as defined in Eq. (1), with $r_o=126$ [$\$/m^3$], $r_w=19$ [$\$/m^3$] and $r_i=6$ [$\$/m^3$].

Using the reactive approach, each production well is simply shut in if production is no longer profitable, where the profitability threshold corresponds to a watercut of 87%. The injection flow rates and production flow rates are fixed at 24 [m^3/day] and 48 [m^3/day] respectively. However, when a production well is shut in, the injection rate of each injection well is proportionally scaled down in order to meet Eq. (14). Due to its reactive nature, the strategy does not require any assumption on the geological structure of the reservoir. Hence, this strategy will be treated as a benchmark to the remaining optimal control strategies that need a predictive reservoir model or models to determine a strategy. The reactive control strategy is applied to each of the 100 members of the set of realizations, resulting in 100 values of the objective function (1).

The nominal optimization approach is based on a single realization, which is assumed to be the "best guess". We select realization number 1 as the basis on which to determine the nominal optimal control strategy, however any of the 100 realizations would be a fair choice as they are assumed equiprobable.

TABLE 2 - RESULTS

	reactive control	nominal optimization		robust optimization	
minimal *NPV*	40,7 M$	43,4 M$	+6,6%	45,0 M$	+10,6%
maximal *NPV*	46,5 M$	49,1 M$	+5,6%	49,4 M$	+6,2%
expected *NPV*	43,8 M$	46,5 M$	+6,2%	47,8 M$	+9,1%

The strategy is determined using the gradient-based optimization procedure and requires little over 3 hours to converge to the optimal solution on a single computer. The resulting production strategy is subsequently applied to the 100 realizations resulting in 100 values of the objective function.

The robust optimization approach uses the entire set of realizations to determine a control strategy that maximizes the expected NPV over the entire set of realizations. The robust optimal control strategy is determined using the same gradient-based optimization procedure as in the nominal optimization approach. However, calculating the "robust" gradient information requires calculating the gradients for each realization individually. Hence, the simulation time is about 100 times longer than the time needed for the nominal optimization approach, i.e. approximately 2 weeks.

Each of the three approaches results in 100 values of the objective function. From these values the minimum, maximum and mean value is calculated as presented in Table 2. Furthermore, 3 cumulative distribution functions are determined, based on these values, as depicted in Fig. 3.

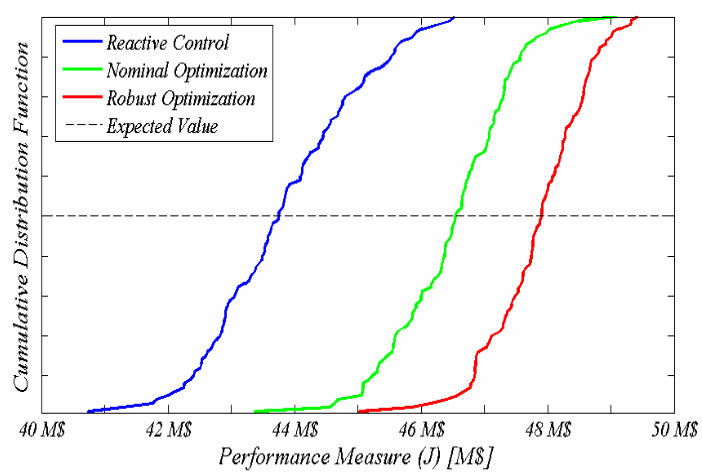

Fig. 3: Cumulative Distribution Functions of three different control strategies: Reactive Control, Nominal Optimization and Robust Optimization, based on the resulting NPV's of each realization in a set of 100.

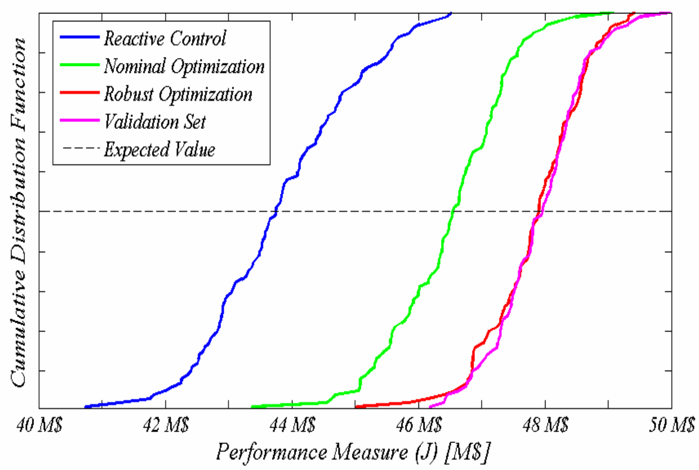

Fig. 4: Cumulative Distribution Functions, showing the added distribution function based on the the NPV's resulting from applying the robust optimization strategy to an extra set of 100 alternative realizations.

Compared to the reactive approach, the nominal strategy results in a major improvement of *8,8%* on the NPV of realization number 1 (on which the optimal strategy is based) . However, if one applies the nominal strategy to the entire set of realizations, which reflect the geological uncertainty, the expected improvements are less profound, as can be observed in Table 2. It shows that the expected NPV is *6.2%* higher than the expected NPV using a reactive approach, but this is less than what one would expect based on an evaluation of the single model only.

Fig. 3 and Table 2 also show that the robust optimization strategy results in a higher expected NPV compared to the nominal optimization strategy and the reactive control strategy. As the objective to the robust optimization procedure is the maximization of the expected NPV, this is not unexpected and indicates that the procedure is successful.

Finally, although no claims were made on the range of possible NPV's, the cumulative distribution function of the robust optimization approach has a smaller distribution of NPV's compared to the other two methods. This reduction in variance is obviously an advantageous quality, as it provides more certainty within the decision process whether or not to exploit a particular oil reservoir.

Validation

The robust optimization strategy derived based on the set of realizations provides a significant improvement of the expected NPV and range of possible NPV values. However, robustness can truly be claimed if these good results also hold for any realization which is outside the set used, but is also within the boundaries laid out by the geological uncertainty.

In order to validate "robustness" we have generated an alternative set of 100 different realizations in correspondence with the properties of the geological uncertainty. Subsequently we applied the robust control strategy to this alternative set of realizations. The resulting NPV's are again used to determine a cumulative distribution function which is presented in Fig. 4.

Fig. 4 shows clearly that the results of the robust optimization strategy, applied to the second set of realization produces an almost identical cumulative distribution function as the initial one. This shows that the robust optimization strategy does in fact introduce robustness to the impact of geological uncertainty on the NPV in this example

Conclusion

A robust optimization technique is an attractive approach to oil recovery optimization problems, as it creates a bridge between two research fields within the E&P industry: dealing with geological uncertainty and maximizing oil recovery revenues. The results following from the motivating example point out that a robust optimization procedure is able to improve the expected NPV significantly and results in a smaller range of possible NPV outcomes Besides this, the expected NPV and range of outcomes seem to hold for the entire range of possible geological scenarios which correspond to the uncertainty.

Within this work, injection and production flow rates are used to manipulate the progression of the oil-water front in the reservoir. The equality constraint, resulting from using flow rate control, limits the search space of the optimization algorithm. Incorporating a well model into the system of adjoint equations allows for the optimization to be carried out over the control valve settings. Using these valve settings, the use of an additional equality constraint is no longer necessary.

No measurement information is assumed available, within this study. Additional measurement information can however be used to reduce the geological uncertainty associated within the reservoir model. In future research on robust optimization of reservoir flooding, a more integrated approach is advised, in which measurements can be used to narrow the set of realizations or estimate the probability of each realization.

Nomenclature

Reservoir Modelling

p	*pressure*	$[Pa]$
S	*saturation*	[-]
Φ	*porosity*	[-]
μ	*viscosity*	$[Pa\ s]$
ρ	*density*	$[kg/m^3]$
q	*flow rate*	$[m^3/day]$
w	*well constant*	$[m/Pa\ s]$
$_o$	*oil*	[-]
$_w$	*water*	[-]
$_i$	*injection*	[-]

Optimization

J	*performance measure*
$\bar{J}$	*average performance measure*
q	*control vector (flow rates)*
q_{min}	*minimum flow rate*
q_{max}	*maximum flow rate*
x	*state vector*
x_0	*initial condition*
H	*Hamiltonian*
λ	*adjoint vector*
k	*time index*

N	*number of time steps*
N_R	*number realizations*
τ	*step size SD algorithm*
d	*feasible gradient vector*

References

1. D.R. Brouwer and J.D. Jansen: "Dynamic optimization of water flooding with smart wells using optimal control theory", *SPEJ*, vol. 9, 2004, pp 391-402.
2. L. Landa and R.N. Horne: "A procedure to integrate well test data, reservoir performance history and 4-D seismic information into a reservoir description", paper SPE Annual Technical Conference and Exhibition, 1997.
3. R. Li, A.C. Reynolds and D.S. Oliver: "History matching of three-phase flow production data", *SPEJ*, vol. 8, issue 4, 2003, pp 328-340
4. J.D. Jansen, D.R. Brouwer, G. Naevdal, and C.P.J.W. van Kruijsdijk: "Closed-loop reservoir management", *First Break*, vol. 23, 2005, pp 43-48.
5. B. Srinivasan, D. Bonvin, E. Visser and S. Palanki: "Dynamic optimization of batch processes: II. Role of measurements in handling uncertainty", *Computers & Chemical Engineering*, vol. 27, issue 1, 2003, pp 27-44.
6. P. Terwiesch, D. Ravemark, B. Schenker, and D.W.T. Rippin: "Semi-batch process optimization under uncertainty: Theory and experiments", *Computers & Structures,* vol. 79, issue 1, 1998, pp 77-86.
7. D. Ruppen, C. Benthack, and D. Bonvin: "Optimization of batch reactor operation under parametric uncertainty - computational aspects", *Journal of Process Control*, vol. 5, issue 4, 1995, pp 235-240.
8. B. Yeten, L.J. Durlofsky, and K. Aziz , "Optimization of Smart Well Control", paper SPE International Thermal Operations and Heavy Oil Symposium and International Horizontal Well Technology Conference, 2002
9. P. Sarma, K. Aziz, and L.J. Durlofsky, "Implementation of Adjoint Solution for Optimal Control of Smart Wells", paper SPE Reservoir Simulation Symposium, 2005.
10. P. Sarma, W.H. Chen, L.J. Durlofsky and K. Aziz, "Production Optimization With Adjoint Models Under Nonlinear Control-State Path Inequality Constraints", paper Intelligent Energy Conference and Exhibition, 2006
11. D.G. Luenberger: "Linear and Nonlinear Programming", Second Edition, Addison-Wesley, 1984.
12. Strebelle, S.: "Sequential Simulation Drawing Structures from Training Images", *Ph.D. thesis*, Stanford University, 2000.
13. D.E. Kirk, "Optimal Control Theory, an introduction", Prentice-Hall, 1970.
14. J. Caers, S. Strebell, and K. Payrazyan: "Stochastic integration of seismic data and geologic scenarios", *The Leading Edge*, vol. 22, 2003, pp 192-196.

Appendix A – Gradient calculation using system of adjoint equations

The dynamic reservoir model can be described by the following state-space formulation:

$$\boldsymbol{V}(\boldsymbol{x}_k)\cdot\boldsymbol{x}_{k+1} = \boldsymbol{T}(\boldsymbol{x}_k)\cdot\boldsymbol{x}_k + \boldsymbol{q}_k, \quad \boldsymbol{x}_0 = given \;\ldots\ldots\ldots\ldots\ldots(10)$$

where $\boldsymbol{x}_k$ denotes the state variables with elements corresponding to oil pressures and water saturations in all grid blocks at time step index k. The matrix $\boldsymbol{V}(\boldsymbol{x}_k)$ contains the storage terms and $\boldsymbol{T}(\boldsymbol{x}_k)$ the transmissibility terms[1].

The injection and production rates are subject to inequality constraints as they are bounded by a minimum ($\boldsymbol{q}_{min}$) and maximum ($\boldsymbol{q}_{max}$) rate. Secondly, an additional equality constraint is implemented, stating that the total injection rate ($\boldsymbol{q}_i$) must equal the total production rate ($\boldsymbol{q}_o + \boldsymbol{q}_w$) at each time step k, meant to keep the reservoir pressure constant. It is introduced within the optimal control problem to avoid a gas breakout if the reservoir pressure decreases below bubble-point pressure. This results in the following mathematical formulation:

$$\max_{\boldsymbol{q}} J(\boldsymbol{q}) = \max_{\boldsymbol{q}} \sum_{k=1}^{K} L(\boldsymbol{x}_k,\boldsymbol{q}_k), \;\ldots\ldots\ldots\ldots\ldots\ldots\ldots\ldots\ldots(11)$$

$$s.t. \quad \boldsymbol{x}_{k+1} = F\left(\boldsymbol{x}_k,\boldsymbol{q}_k\right), \quad \boldsymbol{x}_0 = given, \;\ldots\ldots\ldots\ldots\ldots\ldots(12)$$

$$\boldsymbol{q}_{min} \le \boldsymbol{q}_k \le \boldsymbol{q}_{max}, \;\ldots\ldots\ldots\ldots\ldots\ldots\ldots\ldots\ldots\ldots\ldots(13)$$

$$\boldsymbol{q}_{o,k} + \boldsymbol{q}_{w,k} = \boldsymbol{q}_{i,k}, \;\ldots\ldots\ldots\ldots\ldots\ldots\ldots\ldots\ldots\ldots\ldots(14)$$

where F represents the system equations as described in Eq. (10), L represents the integral part of the performance measure (1) and x_0 is a vector containing the initial conditions.

Various approaches to dynamic optimization problems exist, from which we evaluate four to be applied to the optimization of the oil recovery: a gradient-based method, a shooting method, a simultaneous method and dynamic programming[8]. The latter two are not able to deal with large-scale systems and are therefore not suitable to handle complex reservoir models. Both a shooting method as a gradient-based method can handle large-scale models. However, a shooting method may experience stability problems in solving the required system of adjoint equations. For this reason, a gradient-based optimization procedure is implemented within this work.

The gradients of the performance measure J towards the flow rates $\boldsymbol{q}$, to be used within the optimization procedure, are obtained using a system of adjoint equations $\boldsymbol{\lambda}$. In order to use the adjoint variables to obtain the gradients, the *Hamiltonian* function H needs to be determined. The Hamiltonian function at time step k, in which the equality (14) and inequality constraint (13) are discarded, is defined as follows:

$$H_k = L(\boldsymbol{x}_k,\boldsymbol{q}_k) + \boldsymbol{\lambda}_k^T \cdot F(\boldsymbol{x}_k,\boldsymbol{q}_k), \;\ldots\ldots\ldots\ldots\ldots\ldots\ldots\ldots(15)$$

where $\boldsymbol{\lambda}$ is a vector containing the adjoint variables, which are obtained by integrating the adjoint equations backward in time after integrating the system equations forward in time:

$$\boldsymbol{\lambda}_{k-1} = \left.\frac{\partial L}{\partial \boldsymbol{x}}\right|_k + \boldsymbol{\lambda}_k^T \cdot \left.\frac{\partial F}{\partial \boldsymbol{x}}\right|_k, \quad \boldsymbol{\lambda}_K^T = 0. \qquad (16)$$

The state and adjoint variables are subsequently used to obtain the gradients of H towards the injection and production rates q:

$$\left.\frac{\partial H}{\partial \boldsymbol{q}}\right|_k = \left.\frac{\partial L}{\partial \boldsymbol{q}}\right|_k + \boldsymbol{\lambda}_k^T \left.\frac{\partial F}{\partial \boldsymbol{q}}\right|_k \qquad (17)$$

Subsequently, the gradients $\left.\frac{\partial H}{\partial \boldsymbol{q}}\right|_k$ can easily be reformulated into $\left.\frac{\partial J}{\partial \boldsymbol{q}}\right|_k$:

$$\left.\frac{\partial J}{\partial \boldsymbol{q}}\right|_k = \left.\frac{\partial H}{\partial \boldsymbol{q}}\right|_k \cdot \Delta t_k \qquad (18)$$

Thus, the gradients $\frac{\partial J}{\partial q}$ are given by:

$$\frac{\partial J}{\partial \boldsymbol{q}} = \left[\left.\frac{\partial J}{\partial \boldsymbol{q}}\right|_1 \quad \left.\frac{\partial J}{\partial \boldsymbol{q}}\right|_2 \quad \cdots \quad \left.\frac{\partial J}{\partial \boldsymbol{q}}\right|_K \right]. \qquad (19)$$